Acta Crystallographica Section D
Biological Crystallography
ISSN 0907-4449

Structure of nondiscriminating glutamyl-tRNA synthetase from *Thermotoga maritima*

Takuhiro Ito,[a,b] Noriko Kiyasu,[c] Risa Matsunaga,[c] Seizo Takahashi[c] and Shigeyuki Yokoyama[a,b]*

[a]Department of Biophysics and Biochemistry, Graduate School of Science, The University of Tokyo, 7-3-1 Hongo, Bunkyo-ku, Tokyo 113-0033, Japan, [b]RIKEN Systems and Structural Biology Center, 1-7-22 Suehiro-cho, Tsurumi-ku, Yokohama-shi, Kanagawa 230-0045, Japan, and [c]Department of Chemical and Biological Sciences, Faculty of Science, Japan Women's University, 2-8-1 Mejirodai, Bunkyo-ku, Tokyo 112-8681, Japan

Correspondence e-mail: yokoyama@biochem.s.u-tokyo.ac.jp

Received 5 March 2010
Accepted 21 May 2010

PDB Reference: nondiscriminating glutamyl-tRNA synthetase, 3afh.

Aminoacyl-tRNA synthetases produce aminoacyl-tRNAs from the substrate tRNA and its cognate amino acid with the aid of ATP. Two types of glutamyl-tRNA synthetase (GluRS) have been discovered: discriminating GluRS (D-GluRS) and nondiscriminating GluRS (ND-GluRS). D-GluRS glutamylates $tRNA^{Glu}$ only, while ND-GluRS glutamylates both $tRNA^{Glu}$ and $tRNA^{Gln}$. ND-GluRS produces the intermediate Glu-$tRNA^{Gln}$, which is converted to Gln-$tRNA^{Gln}$ by Glu-$tRNA^{Gln}$ amidotransferase. Two GluRS homologues from *Thermotoga maritima*, TM1875 and TM1351, have been biochemically characterized and it has been clarified that only TM1875 functions as an ND-GluRS. Furthermore, the crystal structure of the *T. maritima* ND-GluRS, TM1875, was determined in complex with a Glu-AMP analogue at 2.0 Å resolution. The *T. maritima* ND-GluRS contains a characteristic structure in the connective-peptide domain, which is inserted into the catalytic Rossmann-fold domain. The glutamylation ability of $tRNA^{Gln}$ by ND-GluRS was measured in the presence of the bacterial Glu-$tRNA^{Gln}$ amidotransferase GatCAB. Interestingly, the glutamylation efficiency was not affected even in the presence of excess GatCAB. Therefore, GluRS avoids competition with GatCAB and glutamylates $tRNA^{Gln}$.

1. Introduction

The accuracy of aminoacyl-tRNA formation is an important basis for the fidelity of translation. The aminoacyl moiety in the aminoacyl-tRNA is directly incorporated into the elongating polypeptide on the ribosome. Aminoacyl-tRNA synthetases (aaRSs) catalyze the aminoacylation of the substrate tRNA with the cognate amino acid (Ibba *et al.*, 2005). aaRSs utilize various mechanisms to achieve the required fidelity, *e.g.* precise recognition of the substrate amino acid in the catalytic pocket, strict recognition of the identity element in the substrate tRNA and hydrolysis of misacylated products by the 'editing' domain. Most bacteria and all archaea utilize GluRS to glutamylate both $tRNA^{Glu}$ and $tRNA^{Gln}$ and do not possess a glutaminyl-tRNA synthetase. This type of GluRS is called a nondiscriminating (ND) GluRS. The correctly produced Glu-$tRNA^{Glu}$ is directly used in translation, while the misacylated intermediate Glu-$tRNA^{Gln}$ is converted to Gln-$tRNA^{Gln}$ by a Glu-$tRNA^{Gln}$ amidotransferase before being used in translation (Wilcox & Nirenberg, 1968). In bacteria, the heterotrimeric enzyme GatCAB, which consists of GatA, GatB and GatC, functions as a Glu-$tRNA^{Gln}$ amidotransferase (Curnow *et al.*, 1997).

© 2010 International Union of Crystallography
Printed in Singapore – all rights reserved

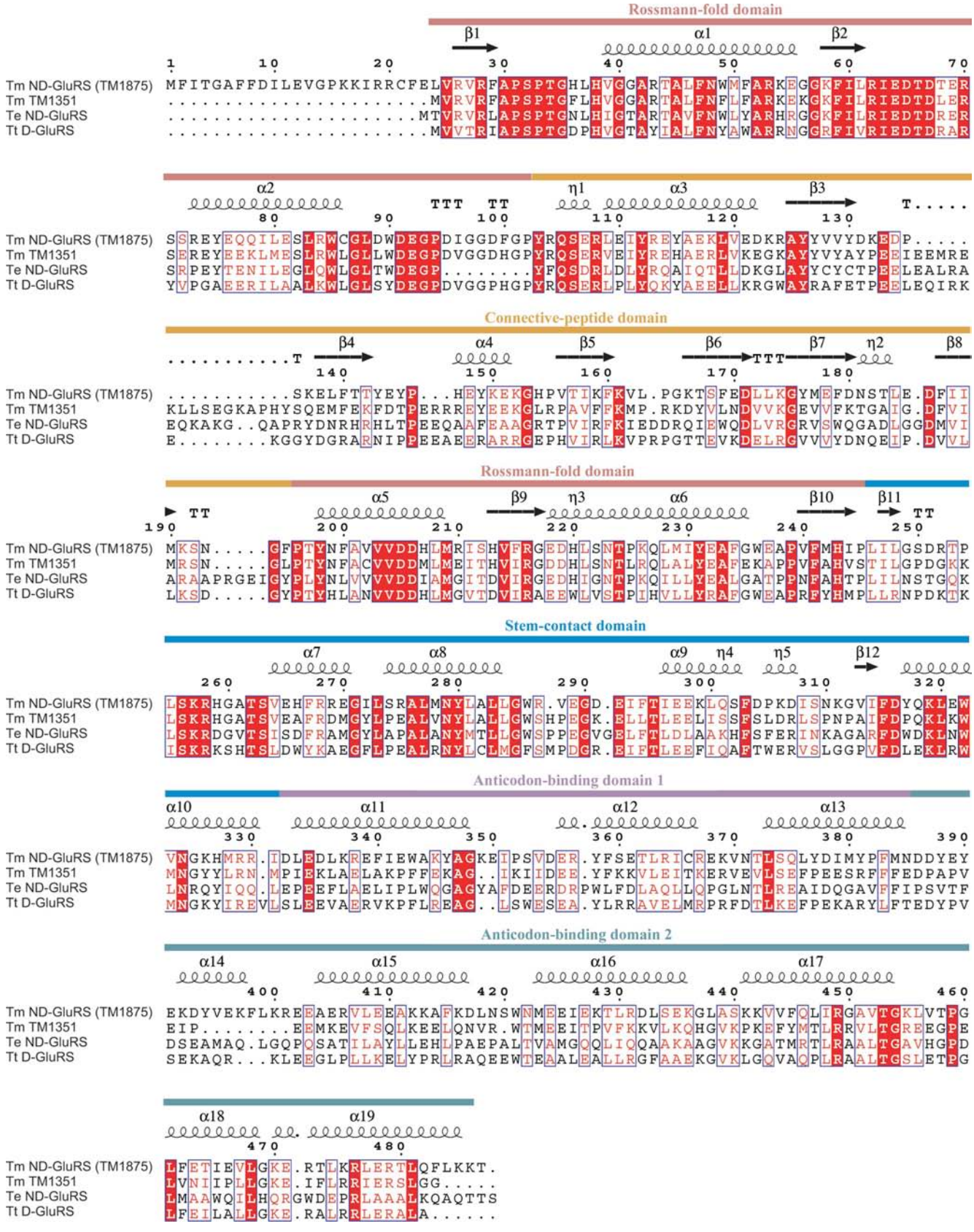

Figure 1
Sequence alignment of *T. maritima* (Tm) ND-GluRS (TM1875), Tm TM1351, *Thermosynechococcus elongatus* (Te) ND-GluRS and *Thermus thermophilus* (Tt) D-GluRS. The amino-acid sequences were aligned using the program *ClustalW* (Larkin *et al.*, 2007) and were illustrated using the program *ESPript* (Gouet *et al.*, 1999). The domain structures and the secondary-structural elements of Tm ND-GluRS are indicated above the sequences. Conserved and similar residues are highlighted by red boxes and red letters, respectively.

Table 1
Data-collection and refinement statistics.

Values in parentheses are for the last shell.

Data collection	
Wavelength (Å)	1.0000
Resolution (Å)	50.00–2.00 (2.07–2.00)
Space group	$P2_12_12$
Unit-cell parameters (Å)	a = 68.6, b = 207.3, c = 39.5
Observed reflections	240286
Unique reflections	37578
Redundancy	6.4 (4.8)
Completeness (%)	95.7 (72.0)
$I/\sigma(I)$	17.9 (2.2)
R_{merge} (%)	9.5 (40.2)
Refinement	
Resolution (Å)	50.00–2.00
No. of reflections used	37512
Working set	35646
Test set	1866
No. of non-H atoms	
Protein	3856
Ligand	32
Water	516
Mean B values (Å^2)	
Protein	28.9
Ligand	20.7
Water	39.3
R_{work} (%)	18.7
R_{free} (%)	23.5
R.m.s.d.s from ideal geometry	
Bond lengths (Å)	0.008
Bond angles (°)	1.23
Ramachandran plot (%)	
Most favoured	93.5
Additional allowed	6.5

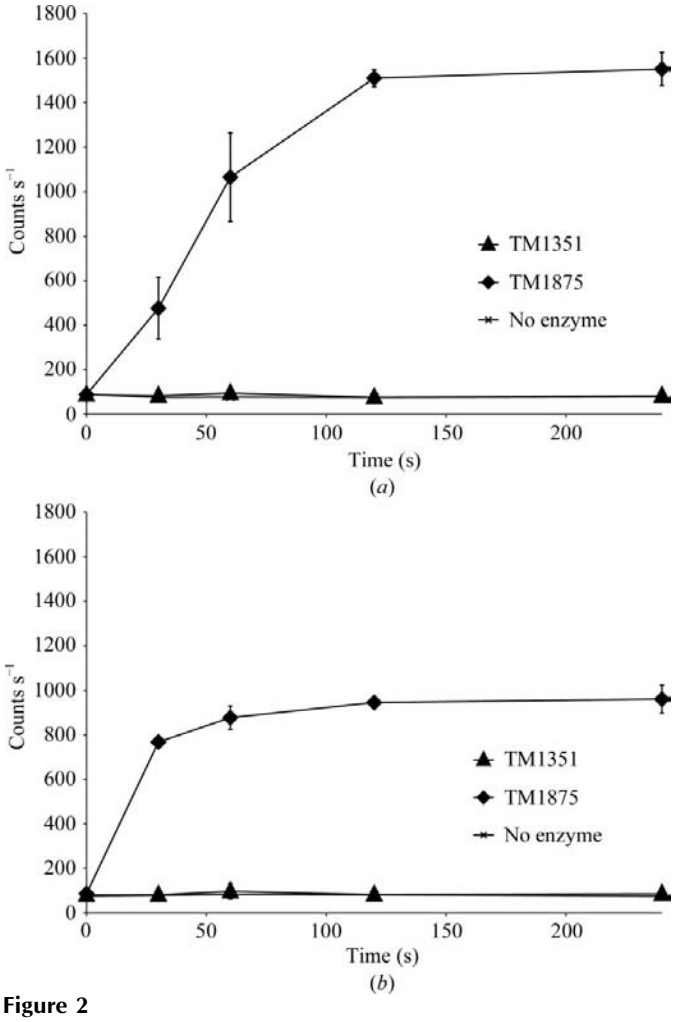

Figure 2
Aminoacylation by TM1875 and TM1351. The glutamylation of (*a*) $tRNA^{Glu}_{CUC}$ and (*b*) $tRNA^{Gln}_{CUG}$ by TM1875 (diamonds) and TM1351 (triangles) was analyzed. The *x* and *y* axes represent the reaction time for glutamylation and the incorporated radioactivity, respectively.

Several bacterial species possess two ND-GluRSs, called GluRS1 and GluRS2 (Salazar *et al.*, 2003; Skouloubris *et al.*, 2003). GluRS1 and GluRS2 in *Helicobacter pylori* reportedly prefer $tRNA^{Glu}$ and $tRNA^{Gln}$, respectively (Skouloubris *et al.*, 2003). In *Thermotoga maritima*, two genes encoding GluRS (TM1351 and TM1875) have been identified, but their biochemical characteristics have not been analyzed (Salazar *et al.*, 2003; Skouloubris *et al.*, 2003).

In this study, we tested TM1351 and TM1875 for their aminoacylation activities against the $tRNA^{Glu}$ and $tRNA^{Gln}$ transcripts and clarified that only TM1875 functions as an ND-GluRS. In addition, we determined the crystal structure of TM1875, the *T. maritima* ND-GluRS, at 2.0 Å resolution. Structural comparisons with other GluRSs revealed several interesting features. We also measured the aminoacylation efficiency of $tRNA^{Gln}$ by ND-GluRS in the presence of GatCAB.

2. Materials and methods

2.1. Sample preparation

All of the genes from *T. maritima* analyzed in this study were obtained by PCR amplification from the genome. The open reading frames encoding TM1875 and TM1351 were cloned into the *Nco*I/*Xho*I sites of pET-28b(+) (Novagen) and the *Nde*I/*Sal*I sites of pET-26b(+) (Novagen), respectively; the expressed proteins lacked purification tags. TM1875 and TM1351 were both purified in the same manner. *Escherichia coli* strain Rosetta2 (DE3) was transformed by the recombinant plasmids and was cultured in LB medium. Protein synthesis was induced by adding isopropyl β-D-1-thiogalactopyranoside (IPTG) to a final concentration of 0.5 m*M*. The transformed *E. coli* cells were cultured at 303 K for 5 h after induction and were harvested. The cells were lysed by sonication and the debris was removed by centrifugation. The lysate was heated at 348 K for 30 min and was centrifuged to remove the precipitated components. The clarified supernatant was purified by ion-exchange column chromatography using RESOURCE Q (GE Healthcare) and by gel-filtration column chromatography using Superdex 200 (GE Healthcare). The purified TM1875 and TM1351 proteins were each dissolved in 20 m*M* Tris–HCl buffer pH 7.0 containing 5 m*M* $MgCl_2$, 10 m*M* 2-mercaptoethanol and 50 m*M* NaCl.

For the expression of *T. maritima* GatCAB, the genes encoding GatC and GatAB were cloned within the *Nco*I/*Bam*HI sites and the *Nde*I/*Eco*RV sites in MCS1 and MCS2, respectively, of pET-Duet-1 (Novagen) to generate pET-Duet-

GatCAB, in which the genes encoding GatA and GatB are tandemly linked in MCS2 in the same manner as in the *T. maritima* genome. Expression and purification of *T. maritima* GatCAB were performed in the same manner as for TM1875, except for the lysis buffer (50 m*M* Tris–HCl buffer pH 7.0 containing 50 m*M* NaCl, 500 m*M* $MgCl_2$ and 10 m*M* 2-mercaptoethanol).

All tRNA transcripts were prepared by *in vitro* transcription with T7 RNA polymerase and the transcribed tRNAs were purified by ion-exchange chromatography using RESOURCE Q (GE Healthcare).

2.2. Aminoacylation assay

The aminoacylation mixtures contained 50 m*M* HEPES–NaOH buffer pH 7.5, 20 m*M* $MgCl_2$, 91.6 µ*M* [^{14}C]-glutamate, 0.8 µ*M* TM1875 (GluRS) or TM1351, 10 µ*M* tRNA and 4 m*M* ATP. Aminoacylation experiments of TM1875 (GluRS) with or without GatCAB (0–15 µ*M*) were also performed in the same manner. The reaction was started by the addition of tRNA and ATP at 323 K and 5 µl aliquots were removed from the tubes at the indicated time points and were placed onto filters containing trichloroacetic acid (TCA) to stop the reaction. The filters were washed with ice-cold 5% TCA and ethanol. The radioactivity of the air-dried filters was counted with a scintillation counter.

2.3. Gel mobility-shift assay

GatCAB alone (20 µ*M*) and 2 µ*M* $tRNA^{Gln}_{CUG}$ transcript with or without 20 µ*M* GatCAB were dissolved in 50 m*M* HEPES–KOH buffer pH 7.5 containing 10 m*M* $MgCl_2$, 20 m*M* KCl, 2 m*M* 2-mercaptoethanol and 10% glycerol. The samples were fractionated on a 7% polyacrylamide gel containing 50 m*M* HEPES–KOH buffer pH 7.5. After electrophoresis, the tRNA bands were detected by SYBR Gold staining (Invitrogen).

2.4. Protein crystallization, data collection and structure determination

TM1875 (ND-GluRS) was concentrated to a final concentration of about 15 mg ml^{-1} for crystallization using an Amicon Ultra filter (Millipore). A 1.8 µl portion of the sample solution, supplemented with 1 m*M* L-glutamyl-sulfamoyl adenosine (Glu-SA), was mixed with 0.4 µl 30% D-sorbitol and 1.8 µl reservoir solution consisting of 100 m*M* HEPES–NaOH buffer pH 7.5, 8% ethylene glycol and 15% PEG 8000. The resulting 4 µl solution was dropped onto a siliconized cover glass, sealed onto a well filled with 500 µl reservoir solution and incubated at 293 K. Rod-like crystals appeared in the drop within one week. The crystals were flash-cooled with liquid nitrogen in a cryoprotectant reagent consisting of 100 m*M* HEPES–NaOH buffer pH 7.5, 50 m*M* NaCl, 5 m*M* $MgCl_2$, 10 m*M* 2-mercaptoethanol, 0.5 m*M* Glu-SA, 3% D-sorbitol, 20% ethylene glycol and 15% PEG 8000.

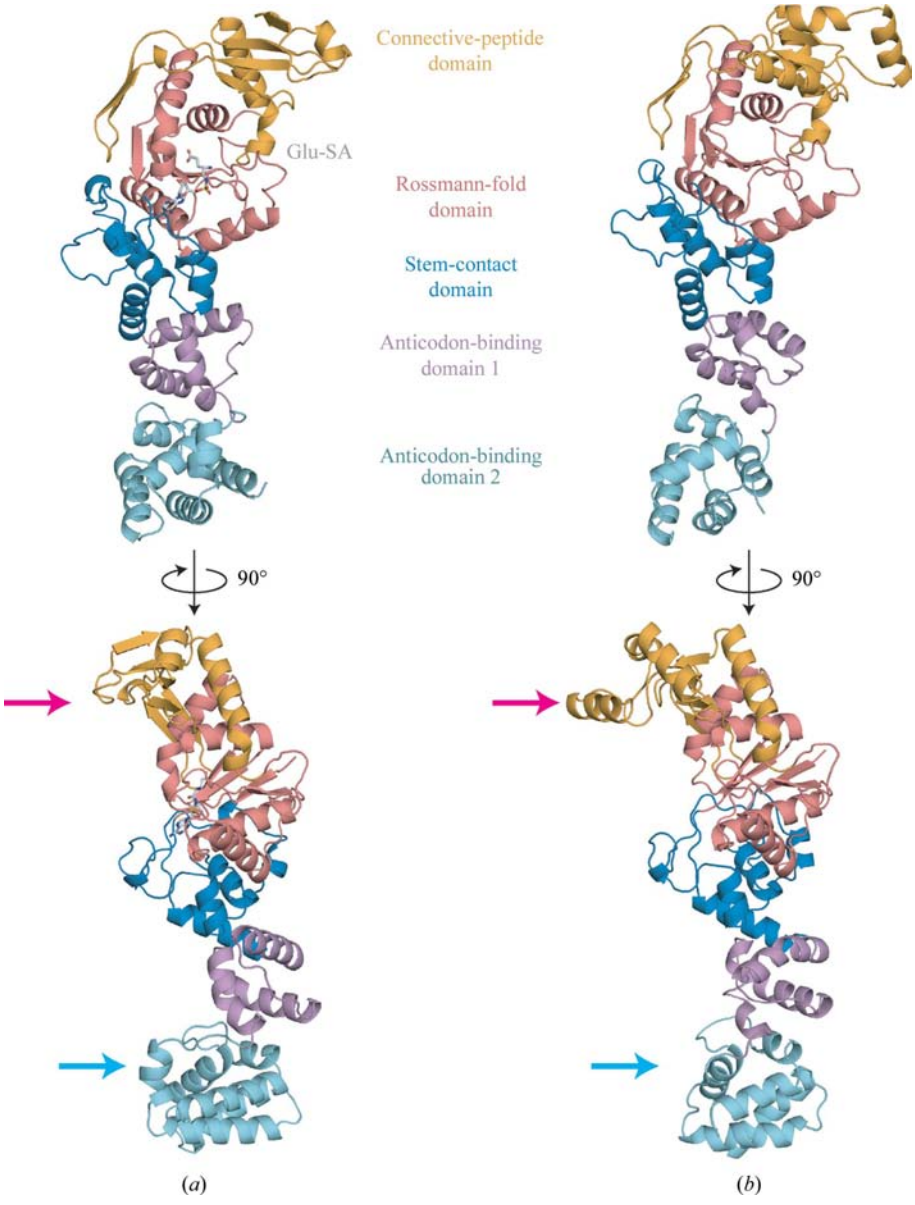

Figure 3
Overall structures of (*a*) *T. maritima* ND-GluRS (TM1875) and (*b*) TM1351 (PDB code 2o5r). The structures of the *T. maritima* ND-GluRS–Glu-SA complex and TM1351, viewed from two vertical directions, are represented as ribbon models. The five domains are coloured differently: Rossmann-fold domain, salmon; connective-peptide domain, orange; stem-contact domain, blue; anticodon-binding domain 1, violet; anticodon-binding domain 2, cyan. The Glu-SA bound in the catalytic pocket is shown as a stick model. All graphical figures were prepared using the program *PyMOL* (DeLano, 2002).

An X-ray diffraction data set was collected on beamline AR-NW12A at the Photon Factory (Ibaraki, Japan). The data set was processed with the *HKL*-2000 software (Otwinowski & Minor, 1997). The initial phases were determined by the molecular-replacement method using the program *Phaser* (McCoy *et al.*, 2007). The tertiary structure of TM1351 (PDB code 2o5r; Joint Center for Structural Genomics, unpublished work) was used as the search model. The starting model was automatically constructed with the program *RESOLVE* (Terwilliger, 2003). The model was further constructed and refined manually using the programs *Coot* (Emsley & Cowtan, 2004) and *CNS* (Brunger, 2007; Brünger *et al.*, 1998). The final model had an $R_{\rm work}$ factor of 18.7% and an $R_{\rm free}$ factor of 23.5%. Structure validation was performed with *PROCHECK* (Laskowski *et al.*, 1993) and 93.5% and 6.5% of the nonglycine and nonproline residues were assigned to the most favoured and additional allowed regions, respectively. The data-set and refinement statistics are shown in Table 1. The atomic coordinates and structure factors have been deposited in the Protein Data Bank under accession code 3afh.

3. Results and discussion

3.1. TM1875 functions as an ND-GluRS

We began this study by analyzing the primary sequences of TM1875 and TM1351, as shown in Fig. 1. The sequences are homologous over the entire region, with 45.4% sequence identity and 59.2% sequence similarity. The sequences in the Rossmann-fold domain are quite highly homologous, with 75.2% identity. The tertiary structure of TM1351 (Fig. 3*b*) has previously been reported by the Joint Center for Structural Genomics (PDB code 2o5r) and its structure is very similar to those of previously determined GluRSs such as *Thermus thermophilus* discriminating (D) GluRS (Nureki *et al.*, 1995). Therefore, both TM1875 and TM1351 were considered to function as GluRSs.

Next, we tested TM1875 and TM1351 for the ability to glutamylate $tRNA^{Glu}_{CUC}$ and $tRNA^{Gln}_{CUG}$ (Fig. 2). TM1875 glutamylated both the $tRNA^{Glu}_{CUC}$ and $tRNA^{Gln}_{CUG}$ transcripts and we concluded that TM1875 functions as an ND-GluRS in *T. maritima*. In contrast, TM1351 did not glutamylate the transcripts in our assay. This inability of TM1351 to function in glutamylation was unexpected, given the high homology between the sequences of TM1875 and TM1351. The function of TM1351 is presently unknown and requires further study.

3.2. Overall structure of *T. maritima* ND-GluRS

We have determined the crystal structure of TM1875, the ND-GluRS from *T. maritima*, at 2.0 Å resolution (Fig. 3*a*). The crystal belonged to space group $P2_12_12$, with unit-cell parameters a = 68.6, b = 207.3, c = 39.5 Å; the asymmetric unit contained one ND-GluRS molecule with one cocrystallized

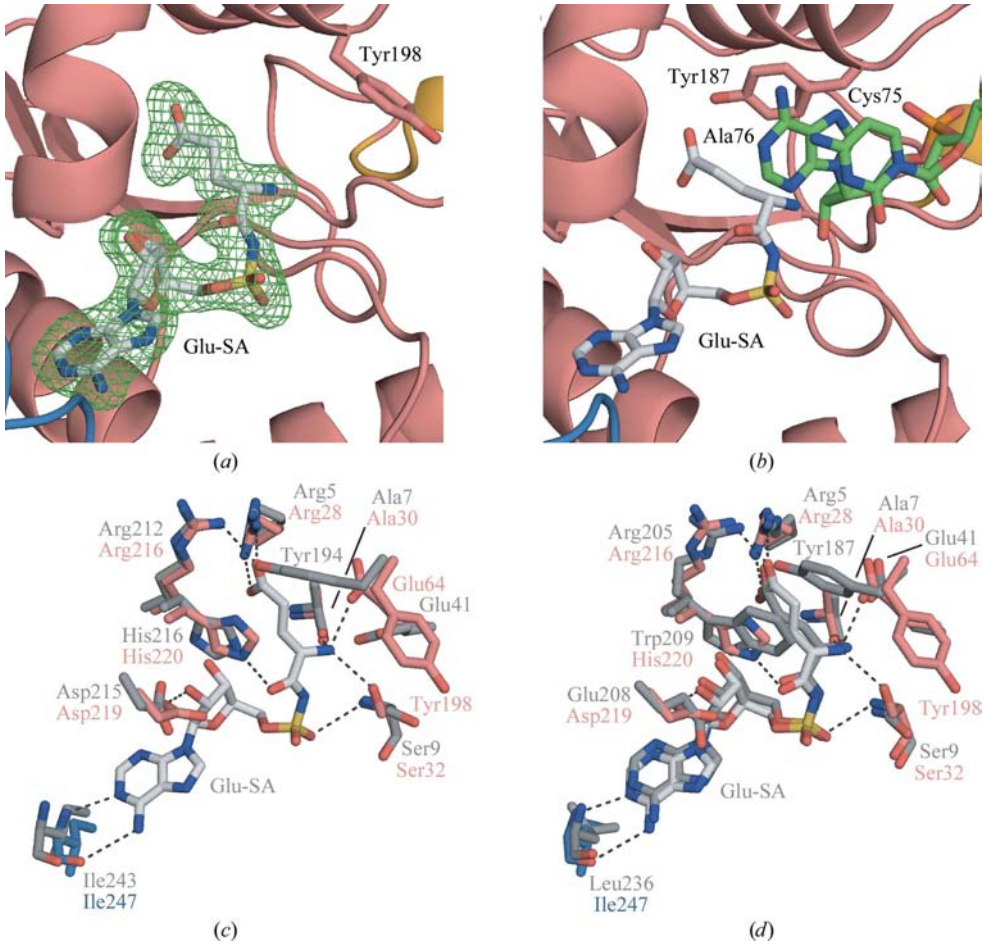

Figure 4
Structural comparison of the catalytic sites of GluRSs. (*a*) Close-up view of Glu-SA in the Tm ND-GluRS–Glu-SA complex. The $|F_o| - |F_c|$ annealed OMIT map of Glu-SA at the 3σ level, in which Glu-SA and the side chain of Tyr198 are represented by stick models. (*b*) Close-up view of Glu-SA in the Tt D-GluRS–$tRNA^{Glu}$–Glu-SA complex. Glu-SA, the tRNA-terminal C75 and A76 nucleotides and the side chain of Tyr187 are represented as stick models. (*c*) Superimposed view of the catalytic sites of Tm ND-GluRS and TM1351. The molecule of Glu-SA (light grey), the residues interacting with Glu-SA in the Tm ND-GluRS–Glu-SA complex (salmon and blue) and the corresponding residues in TM1351 (dark grey) are represented by stick models. The hydrogen bonds identified between Glu-SA and ND-GluRS are indicated by dashed lines. (*d*) Superimposed view of the catalytic sites of the Tm ND-GluRS–Glu-SA complex and the Tt D-GluRS–$tRNA^{Glu}$–Glu-SA complex. The molecules of Glu-SA (light and dark grey for Tm and Tt, respectively) and the residues interacting with Glu-SA in the Tm ND-GluRS–Glu-SA complex (salmon and blue) and the Tt D-GluRS–$tRNA^{Glu}$–Glu-SA complex (dark grey) are represented by stick models.

Glu-SA, a nonhydrolyzable analogue of glutamyl-AMP, in the catalytic pocket. Therefore, the elucidated structure is the ND-GluRS–Glu-SA complex from *T. maritima*. The initial phases were determined by molecular replacement using the structure of TM1351 and the final structural model has an R_{work} factor of 18.7% and an R_{free} factor of 23.5%.

In the elucidated crystal structure, the N-terminal residues up to Glu23 are disordered; therefore, the tertiary structure of the residues from Leu24 to Lys486 was determined. Like other D-GluRSs and ND-GluRSs, the *T. maritima* ND-GluRS consists of five domains: the Rossmann-fold domain, the connective-peptide domain, the stem-contact domain and anticodon-binding domains 1 and 2 (Figs. 1 and 3). The connective-peptide domain is inserted in the Rossmann-fold domain, which is divided into N-terminal and C-terminal parts. Pro102 is located at the domain boundary between the N-terminal part of the Rossmann-fold domain and the connective-peptide domain and has a *cis*-peptide bond.

We compared the tertiary structures of ND-GluRS (TM1875; Fig. 3*a*) and TM1351 (PDB code 2o5r; Fig. 3*b*) and identified two major differences. One is in the connective-peptide domain, as shown by the magenta arrows in Fig. 3. TM1351 possesses a three-turn α-helix, while ND-GluRS has a short β-sheet (β4). This difference is also discussed below in comparison with other GluRSs. The other is in anticodon-binding domain 2, as shown by the cyan arrows in Fig. 3. TM1351 has no helix corresponding to α14 in ND-GluRS. Further studies are required in order to clarify whether these structural variations are related to the differences in the enzymatic activities of ND-GluRS and TM1351.

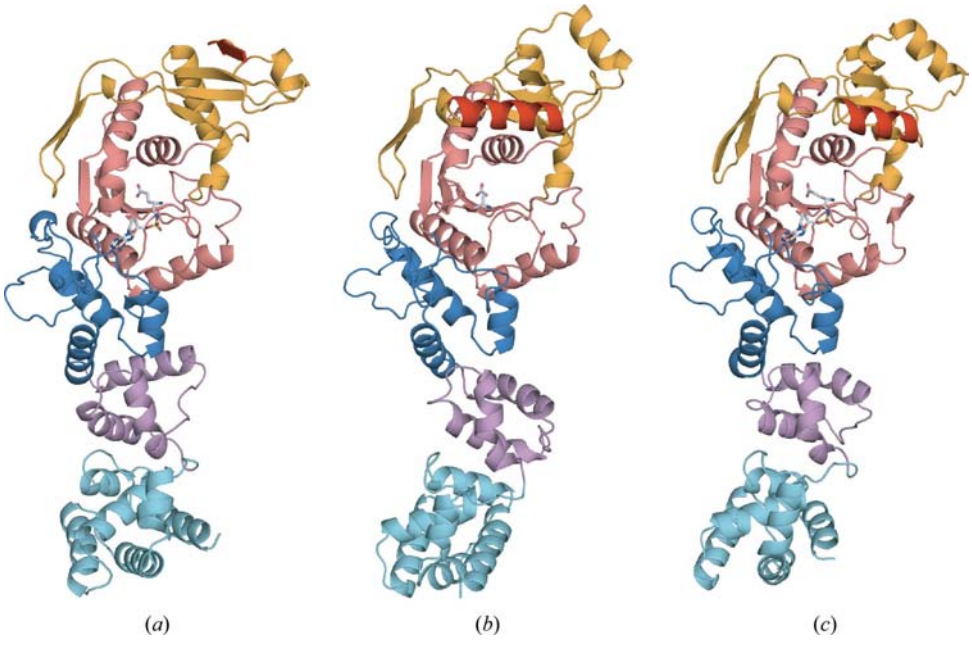

Figure 5
Structural comparison of the GluRSs. The structures of (*a*) the Tm ND-GluRS–Glu-SA complex, (*b*) the Te ND-GluRS–Glu complex and (*c*) the D-GluRS–Glu-SA part of the Tt D-GluRS–tRNA^{Glu}–Glu-SA complex are represented by ribbon models coloured as in Fig. 3. The Glu and Glu-SA molecules in the catalytic pocket are represented by stick models.

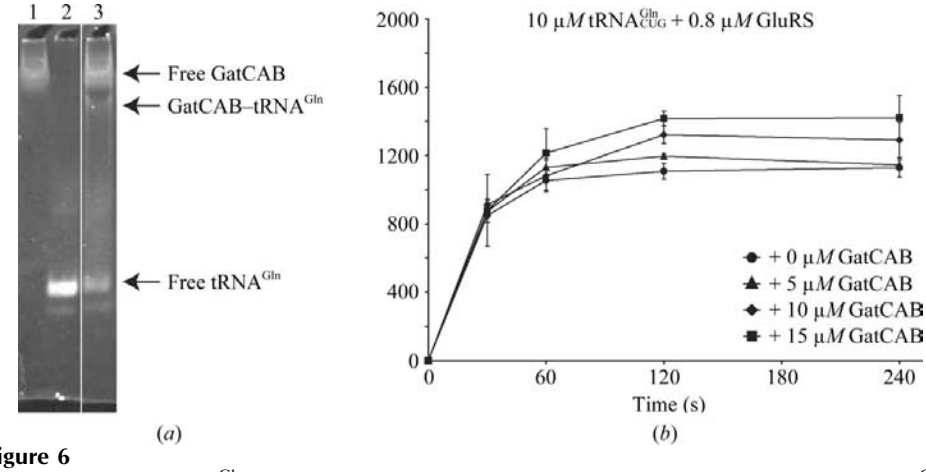

Figure 6
Aminoacylation of tRNA^{Gln} by ND-GluRS in the presence of GatCAB. (*a*) The gel mobility of tRNA$^{Gln}_{CUG}$ was measured in the absence (lane 2) or presence (lane 3) of GatCAB. GatCAB alone was loaded in lane 1 as a control. (*b*) The glutamylation of tRNA$^{Gln}_{CUG}$ by the ND-GluRS was measured in the presence of GatCAB and is represented in the same manner as in Fig. 2. The concentrations of GatCAB are indicated on the graph.

3.3. Structure of the catalytic site

The conformations of the residues within the catalytic site are quite similar in the present *T. maritima* (Tm) ND-GluRS–Glu-SA complex, Tm TM1351 (PDB code 2o5r) and the *Thermus thermophilus* (Tt) D-GluRS–tRNA^{Glu}–Glu-SA complex (PDB code 2cv2; Sekine *et al.*, 2006). However, the χ_1 angles of Tyr198 in the Tm ND-GluRS–Glu-SA complex and the corresponding Tyr187/Tyr194 in the Tt D-GluRS–tRNA^{Glu}–Glu-SA complex/Tm TM1351 are different (Figs. 4*a* and 4*b*). The side chain of Tyr198 in the Tm ND-GluRS–Glu-SA complex points outwards and occupies the CCA-end binding site of the Tt D-GluRS–tRNA^{Glu}–Glu-SA complex.

Surprisingly, the residues that interact with Glu-SA in Tm ND-GluRS are fully conserved in TM1351 (Fig. 4*c*), although the conformations of the above-mentioned tyrosine residues (Tyr198 in ND-GluRS and Tyr194 in TM1351) are different from each other. The perfect conservation of the amino-acid residues

implies that the structural reason for the inability of TM1351 to function in the glutamylation of tRNA may exist in regions of TM1351 other than the catalytic site.

The overall conformation of Glu-SA in the catalytic site is similar to that of Glu-SA in the Tt D-GluRS–tRNA^{Glu}–Glu-SA complex, although the conformation of the glutamyl moiety of Glu-SA is slightly different with respect to the position of the C$^{\gamma}$ atom (Figs. 4*a*, 4*b* and 4*d*). This slight conformational change of the glutamyl moiety may be a consequence of the conformational change of the tyrosine residue described above. The χ_1 angle of this tyrosine residue may alternate between the aforementioned two states in the tRNA-free form and the binding of the CCA end of tRNA probably fixes the χ_1 angle, as in the Tt D-GluRS–tRNA^{Glu}–Glu-SA complex. When the CCA end is bound to the catalytic pocket, the conformation of the glutamyl moiety of Glu-SA may also be fixed.

3.4. Structural comparison with other GluRSs

To date, the crystal structures of three GluRSs have been reported: Tm ND-GluRS, *Thermosynechococcus elongatus* (Te) ND-GluRS (Schulze *et al.*, 2006) and Tt D-GluRS (Nureki *et al.*, 1995; Sekine *et al.*, 2001, 2006). We compared the tertiary structures (Fig. 5) and primary structures (Fig. 1) with those of the present Tm ND-GluRS structure. The overall tertiary structure of Tm ND-GluRS is quite similar to those of Tt D-GluRS (PDB code 2cv2) and Te ND-GluRS (PDB code 2cfo). However, two interesting major differences among the GluRSs were identified.

Firstly, a structural difference is found in the connective-peptide domain. In Tm ND-GluRS the β4 strand comprises the parallel β-sheet together with the β3, β5 and β8 strands (coloured red in Fig. 5*a*). In contrast, in Te ND-GluRS and Tt D-GluRS the corresponding β-strand is replaced by an α-helix, which is also present in Tm TM1351. The structure of this α-helix looks like a gate for the tRNA acceptor stem of the Rossmann-fold domain (coloured red in Figs. 5*b* and 5*c*). Secondly, in anticodon-binding domain 2 the domain orientations relative to the other domains differ among the three GluRSs (coloured cyan in Fig. 5), although their primary and tertiary structures are relatively conserved (Fig. 1). The meaning of these differences requires further study.

3.5. tRNA^{Gln} glutamylation by ND-GluRS in the presence of GatCAB

The intermediate Glu-tRNA^{Gln} produced by ND-GluRS should be converted to Gln-tRNA^{Gln} by a Glu-tRNA^{Gln} amidotransferase. In bacteria, the heterotrimeric enzyme GatCAB is responsible for this reaction (Curnow *et al.*, 1997). Firstly, we used a gel mobility-shift assay to assess whether *T. maritima* GatCAB possesses the ability to bind to *T. maritima* tRNA$^{Gln}_{CUG}$. Fig. 6(*a*) clearly shows that GatCAB is able to bind to tRNA$^{Gln}_{CUG}$ even when it is not glutamylated. This result is consistent with the previous report that the interaction between GatCAB and tRNA^{Gln} from *Staphylococcus aureus* is quite strong (Nakamura *et al.*, 2006). Therefore, we next examined whether the glutamylation efficiency of tRNA^{Gln} by ND-GluRS is perturbed by the presence of GatCAB *in vitro*.

As shown in Fig. 6(*b*), the glutamylation efficiency of tRNA$^{Gln}_{CUG}$ by ND-GluRS was not reduced even in the presence of an excess amount of GatCAB. This result is interesting because both ND-GluRS and GatCAB are considered to bind to the acceptor arm of tRNA^{Gln} from the minor-groove side and to compete for it. These experimental data imply that GatCAB possesses a mechanism to avoid inhibiting the glutamylation of tRNA^{Gln} by ND-GluRS even if GatCAB tightly binds to the uncharged tRNA^{Gln}.

In this study, we found that TM1875 from *T. maritima* functions as an ND-GluRS. In contrast, TM1351, which is highly homologous to TM1875 and other ND-GluRSs and D-GluRSs, lacked glutamylation activity in our assay. We determined the crystal structure of the ND-GluRS (TM1875) from *T. maritima* at 2.0 Å resolution. The structure revealed several differences from the previously determined structures of GluRSs and TM1351. Furthermore, we found that *T. maritima* ND-GluRS glutamylates tRNA^{Gln} even in the presence of an excess amount of *T. maritima* GatCAB. Further analyses will be required in order to determine the function of TM1351 and to clarify how ND-GluRS glutamylates tRNA^{Gln} in the presence of GatCAB.

We thank Dr Shun-ichi Sekine for fruitful discussions and help with data collection. We are grateful to the staff of beamline AR-NW12A at the Photon Factory for their support during data collection. This study was funded in part by the Targeted Proteins Research Program (TPRP) from the Ministry of Education, Culture, Sports, Science and Technology of Japan (MEXT), a Grant-in-Aid for Scientific Research (KAKENHI) from the Japan Society for the Promotion of Science (JSPS) and MEXT and the Global COE Program (Integrative Life Science Based on the Study of Biosignaling Mechanisms) from MEXT.

References

Brunger, A. T. (2007). *Nature Protoc.* **2**, 2728–2733.
Brünger, A. T., Adams, P. D., Clore, G. M., DeLano, W. L., Gros, P., Grosse-Kunstleve, R. W., Jiang, J.-S., Kuszewski, J., Nilges, M., Pannu, N. S., Read, R. J., Rice, L. M., Simonson, T. & Warren, G. L. (1998). *Acta Cryst.* D**54**, 905–921.
Curnow, A. W., Hong, K., Yuan, R., Kim, S., Martins, O., Winkler, W., Henkin, T. M. & Söll, D. (1997). *Proc. Natl Acad. Sci. USA*, **94**, 11819–11826.
DeLano, W. L. (2002). *PyMOL Molecular Viewer.* http://www.pymol.org.
Emsley, P. & Cowtan, K. (2004). *Acta Cryst.* D**60**, 2126–2132.
Gouet, P., Courcelle, E., Stuart, D. I. & Métoz, F. (1999). *Bioinformatics*, **15**, 305–308.
Ibba, M., Francklyn, C. & Cusack, S. (2005). Editors. *The Aminoacyl-tRNA Synthetases.* Georgetown: Landes Bioscience.
Larkin, M. A., Blackshields, G., Brown, N. P., Chenna, R., McGettigan, P. A., McWilliam, H., Valentin, F., Wallace, I. M., Wilm, A., Lopez, R., Thompson, J. D., Gibson, T. J. & Higgins, D. G. (2007). *Bioinformatics*, **23**, 2947–2948.
Laskowski, R. A., MacArthur, M. W., Moss, D. S. & Thornton, J. M. (1993). *J. Appl. Cryst.* **26**, 283–291.

McCoy, A. J., Grosse-Kunstleve, R. W., Adams, P. D., Winn, M. D., Storoni, L. C. & Read, R. J. (2007). *J. Appl. Cryst.* **40**, 658–674.
Nakamura, A., Yao, M., Chimnaronk, S., Sakai, N. & Tanaka, I. (2006). *Science*, **312**, 1954–1958.
Nureki, O., Vassylyev, D. G., Katayanagi, K., Shimizu, T., Sekine, S., Kigawa, T., Miyazawa, T., Yokoyama, S. & Morikawa, K. (1995). *Science*, **267**, 1958–1965.
Otwinowski, Z. & Minor, W. (1997). *Methods Enzymol.* **276**, 307–326.
Salazar, J. C., Ahel, I., Orellana, O., Tumbula-Hansen, D., Krieger, R., Daniels, L. & Söll, D. (2003). *Proc. Natl Acad. Sci. USA*, **100**, 13863–13868.
Schulze, J. O., Masoumi, A., Nickel, D., Jahn, M., Jahn, D., Schubert, W. D. & Heinz, D. W. (2006). *J. Mol. Biol.* **361**, 888–897.
Sekine, S., Nureki, O., Shimada, A., Vassylyev, D. G. & Yokoyama, S. (2001). *Nature Struct. Biol.* **8**, 203–206.
Sekine, S., Shichiri, M., Bernier, S., Chenevert, R., Lapointe, J. & Yokoyama, S. (2006). *Structure*, **14**, 1791–1799.
Skouloubris, S., Ribas de Pouplana, L., De Reuse, H. & Hendrickson, T. L. (2003). *Proc. Natl Acad. Sci. USA*, **100**, 11297–11302.
Terwilliger, T. C. (2003). *Acta Cryst.* D**59**, 38–44.
Wilcox, M. & Nirenberg, M. (1968). *Proc. Natl Acad. Sci. USA*, **61**, 229–236.